5

*BABAR* Note 216
February 15 1995

# Development of the front end readout for the *BABAR* CsI(Th) calorimeter

C Jessop, D. Briggs, D. Freytag, G. Haller, J. Harris, M. King
H. Marsiske, R. Schindler, R. Wang, W. Wisniewski

SLAC

The development of a front end readout system for the *BABAR* CsI calorimeter is described. The performance requirements are stated and two alternative readout schemes which meet these requirements are investigated.

# 1 Performance Requirements

## 1.1 Electronic Noise Requirement

The resolution of a crystal calorimeter is

$$\frac{\sigma_E}{E} = \frac{a_1}{\sqrt[4]{E}} \oplus \frac{a_2}{\sqrt[2]{E}} \oplus \frac{a_3}{E} \oplus b_1 \oplus b_2 \oplus b_3 \qquad (1)$$

where

$a_1$ The empirically observed low energy behavior. Expected to be approx 1 %

$a_2$ Photon counting statistics. Since the light yield of CsI high this term is negligible over most of the energy range.

$a_3$ Electronics noise

$b_1$ Shower leakage fluctuations $\approx$ 1.0 %

$b_2$ Inter-calibration errors $\approx 0.25$ %

$b_3$ Non-uniformities in the crystal response $\approx 0.5$ %

then

$$\frac{\sigma_E}{E} = \frac{1\%}{\sqrt[4]{E}} \oplus \frac{a_3}{E} \oplus 1.2\% \tag{2}$$

We require that the electronic noise does not dominate the resolution at all energies of interest (20 MeVto 12 GeV ). At 20 MeVthe resolution excluding electronic noise is 2.92% $|times$ 20 MeV= 600 keV. The electronic noise per cluster is then required to be less than 600 keV. A variable sized clustering algorithm has been used for simulation studies based on the CLEO algorithm and it is found that at the lowest energies the number of crystals included in a cluster ($n$) is 5. The electronic noise is composed of two components, a coherent one which arises from pickup and an incoherent one which is due to the thermal and shot noise. The coherent component is minimized with efficient shielding but experience shows that it can never be totally eliminated. The coherent noise is difficult to estimate because it depends on the detector environment. However we may use previous similar detectors to attempt to estimate it. Both CLEO and Crystal barrel observed a coherent noise per crystal of approximately 1/3 of the incoherent noise. Hence if $\alpha$ is the coherent noise we require

$$\sqrt{\sum_n \alpha^2} + \sum_n \frac{\alpha}{3} < 600\,\mathrm{keV} \tag{3}$$

We require an incoherent noise of $\alpha < 150$ keVwith a cluster of 5 crystals.

## 1.2 Reliability Requirements

The crystals and front end readout will be inaccessible other than by disassembly of the detector. Such a major undertaking is not expected until at least 10 years after the commissioning of the detector. We therefore have a stringent reliability requirement that there be no dead crystals after 10 years of running. This results in a dual redundancy for the readout [1].

## 2 General Setup

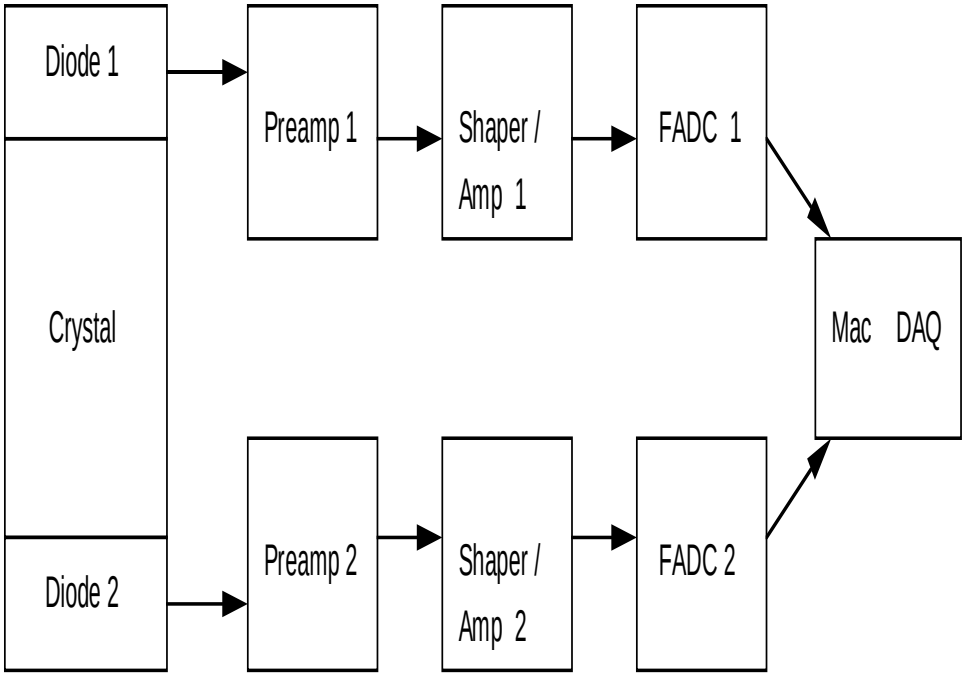


Figure 1: Schematic of front end Readout.

Figure 1 shows a general schematic of a crystal readout scheme. The scintillation light emitted from the crystal when it is irradiated by photons or electrons is sensed by two silicon photodiodes. The photodiodes are coupled to the CsI crystal in two possible ways to be described in subsequent sections. Each photodiode is input to a charge sensitive preamplifier. This is followed by a shaper/post-amplifier. The signal is then digitized using a flash ADC which is read out by an appropriate DAQ system.

The noise performance is usually quoted as equivalent noise energy (ENE). It is dependent on the intrinsic noise of the electronics measured in equivalent noise charge (ENC) and the magnitude of the signal from the photodetector measured in photoelectrons per MeV($L(pe^-/\,\mathrm{MeV})$.

$$ENE(\,\mathrm{keV}) = 10^3 \frac{ENC(e^-)}{L(pe^-/\,\mathrm{MeV})} \tag{4}$$

The signal from the photodetector is related to the photon light yield of the crystals ($L(p/\,\mathrm{MeV})$), the quantum efficiency of the photodetector ($\epsilon_{quant}$), and the efficiency of transmission of light from the crystal to the photodetector ($\epsilon_{trans}$).

$$L(pe^{-}/\,\mathrm{MeV}) = \epsilon_{quant}\epsilon_{trans}L(p/\,\mathrm{MeV}) \tag{5}$$

To achieve low noise therefore requires that not only should the electronics be designed to have low intrinsic noise but that the photodetector should have high efficiency and the light output of the crystal should be maximized.

# 3 Crystal Light Yield

The crystal light yield is strongly dependent on a number of factors. These include the intrinsic properties of the crystal such as thallium doping, the size and geometry of the crystal and the surface preparation and wrapping. There are 58 different sizes for the crystals to be used in the CsI(Th) calorimeter. They vary in length from 29.8 cm to 32.6 cm and are tapered. The cross-section is slightly trapezoidal but may be approximated as a square. The front face varies from $4.7 \times 4.7$ cm$^2$ to $4.9 \times 4.9$ cm$^2$ and the back face from $5.7 \times 5.7$ cm$^2$ to $6.2 \times 6.2$ cm$^2$. We have developed the readout using a variety of crystals of different sizes and shapes from different vendors. However we quote benchmark numbers for a square tapered crystal manufactured by Kharkov. It is 32 cm in length and tapers from $4.5 \times 4.5$ cm$^2$ to $5.8 \times 5.8$ cm$^2$. Kharkov is a candidate vendor for at least part of the CsI(Th) crystals and 30 crystals of this size have been ordered for use in a prototype. The light yield of a crystal varies along it length. This non uniformity can be removed by degrading the surface polish or reflectivity along the length, a process known as compensation. All crystals used are not compensated and for light yield measurements we irradiate the crystal at the front face.

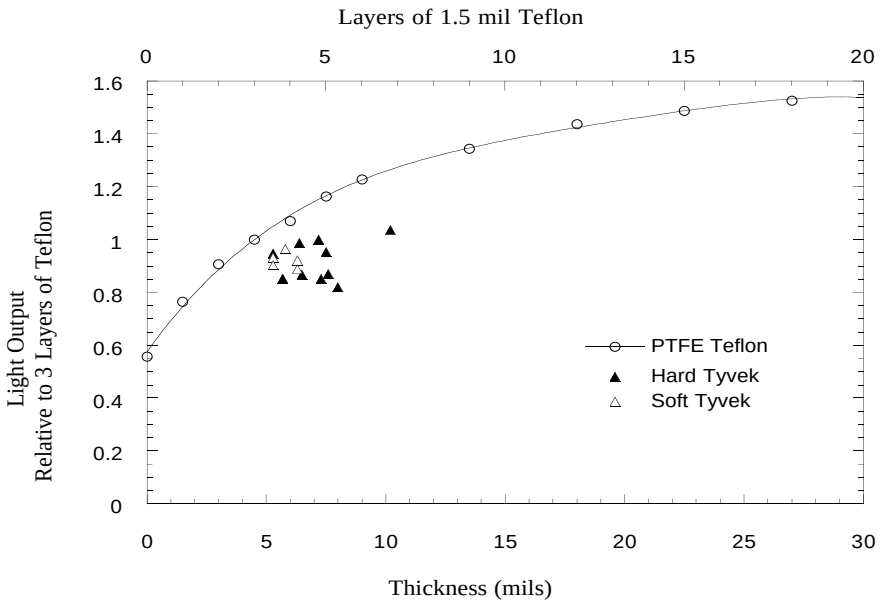


Figure 2: Relative light yield versus number of layers of Teflon [2].

The wrapping of the crystals is constrained by space requirements. If the wrapping is too thick then there is too much space between the crystals so that particles may pass between them without showering or may shower late. The crystal wrapping is constrained to be 150 $\mu$m thick. The crystal must be wrapped in white diffusive reflector. The diffusive nature of the reflector changes the angle of reflection and prevents light from being trapped in the crystal by total internal reflection at the readout face. Two candidate wrappings are Teflon and Tyvek. Figure 2 shows the light yield for the Kharkov crystal versus layers of 38 $\mu$m Teflon [2]. Also shown is the light yield for various thickness of Tyvek. There is only room for 150 $\mu$m of wrapping which allows for three layers of Teflon plus a layer of 25 $\mu$m of aluminum foil. All tests for the readout use only this wrapping. Note that an increased number of layers can considerably boost the light yield and thus the ENE, but any measurements conducted with these conditions are not meaningful for our design.

# 4 Intrinsic Electronic Noise

It is natural to use a silicon photodiode as a photodetector since it is insensitive to magnetic fields, has high quantum efficiency and low noise, can be well matched to the CsI emission spectra, is relatively inexpensive, and has been demonstrated to be highly reliable. There are two options for coupling the diodes to the crystal illustrated in figure 3.

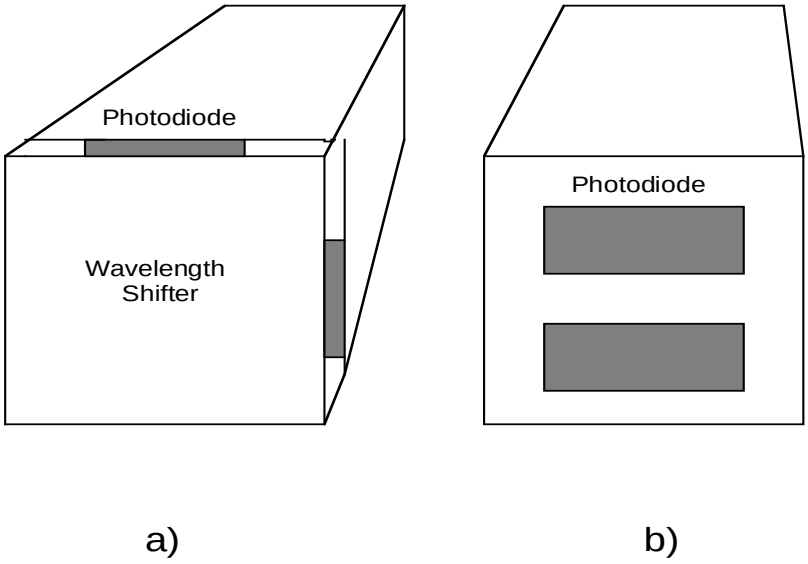


Figure 3: The two different options for coupling the photodiode to the crystal a) Using two $30 \times 3.4$ mm$^2$ photodiodes mounted on the edge of a wavelength shifter. b) Using two $20 \times 10$ mm$^2$ photodiodes mounted directly on the crystal.

The first uses a planar wavelength shifter between the diode and the crystal and the second entails simply epoxying some larger diodes straight to the crystal. Both techniques have been successfully employed at other collider experiments [3] [4]. The wavelength shifting option may offer a substantial improvement in performance at a lower cost than these previous

experiments due to the development of new wavelength shifters while the direct coupling option is a more conservative approach that may only be improved by improvements in diode technology.

In both cases the diodes are read out through a charge sensitive preamplifier. The photodiodes are reversed biased. The preamplifier is a modified version of one that was successfully used in a prototype CsI calorimeter for the Tau/Charm experiment [5]. The intrinsic electronic noise depends on the choice of diodes, preamplifier and shaping used and we now describe this in some detail

# 5 Noise from photodiode/preamplifier

Figure 4 shows the noise equivalent circuit for a silicon photodiode connected to a charge sensitive preamplifier. The diode may be modeled as a capacitor in parallel with a current source. The current $I_d$ is the dark current caused predominantly by impurities in the silicon [6] . The capacitance between the n and p doped layers depends on the depth of the depletion layer d and active area A as.

$$C_d = \frac{\epsilon.A}{d} \tag{6}$$

The best low noise performance is achieved using a discrete n-channel JFET as the input stage to the preamplifier. The FET may be modeled as a series resistance with a parallel capacitance. This is because the JFET is operated as a transconductor ($dI/dV = g_m$) equivalent to a resistance ($R_{JFET} = 1/g_m$). In addition it has an intrinsic capacitance between the gate and source $C_{jfet}$. The preamplifier is followed by a band pass filter which removes high and low frequency noise components and enhances the signal to noise ratio. In its simplest form it consists of a CR-RC shaping network with shaping time $\tau$. The noise of a preamplifier has two components. The first is the current or parallel noise which increases linearly with shaping time. Second is the voltage or series noise which decreases inversely proportional to shaping time. In our case there are two components to the parrallel/current noise. The shot noise of the dark current $I_d$ and the thermal Johnson noise of the total parrallel resistance $R_p$. The parrallel resistance is the bias and feedback resistance of the preamplifier. The series/voltage noise is the thermal noise due to $R_{jfet}$. The voltage noise generates a charge on the overall input

capacitance ($C_d$ + $C_{jfet}$). The equivalent noise charge $\overline{ENC}$ is then

$$ENC^2 = \alpha_1(2qI_d\tau + \frac{4kT}{R_p}\tau) + \alpha_2\frac{8kT(C_{jfet}+C_d)^2}{3g_m\tau} \qquad (7)$$

k is the Boltzman constant, T is the temperature. The two constants $\alpha_1, \alpha_2$ are set by the exact form of the shaping network. In the case of a CR-RC network $\alpha_1 = \alpha_2 = 0.92$. Note that the photodiode dark current is very sensitive to temperature. Cooling by as little as 5-7$^o$C can halve the dark current.

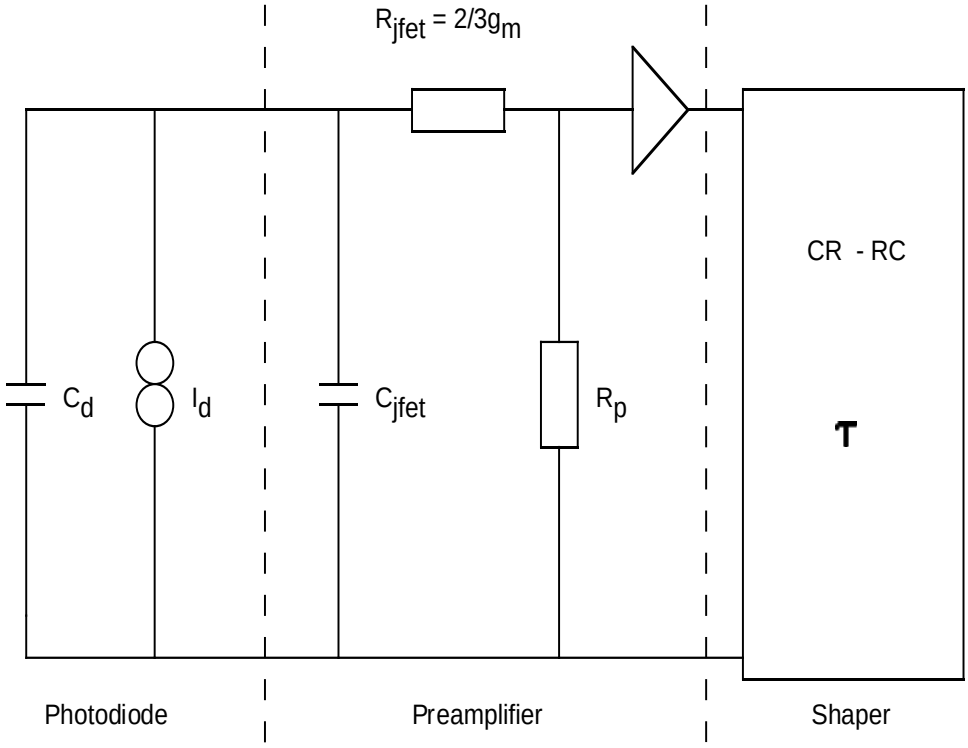


Figure 4: Noise equivalent circuit for front end readout.

# 6 Optimizing the noise performance

It follows from the above considerations that in order to get the best low noise performance.

1. Increase the photon light yield from the crystals $L(p/\,\mathrm{keV})$ (eg. with wrapping etc).
2. Ensure highly efficient transmission of light from the crystal to the photodetector ($\epsilon_{trans}$).
3. Use a photodetector with the highest possible quantum efficiency ($\epsilon_{quant}$).
4. Use a photodetector with the lowest possible dark current ($I_d$) and capacitance ($C_d$). Note that the dark current and the capacitance are dependent on the bias voltage used.
5. Use a JFET with high transconductance ($g_m$) and low intrinsic capacitance ($C_{jfet}$) to minimize the noise.
6. Choose the shaping network and shaping time to minimize the noise (equation 7 has a minima).
7. Ensure adequate shielding and take all precautions to minimize pickup.
8. Cool diodes to minimize the dark current and maintain close control of temperature to keep dark current stable.

We analyze two alternative options for the readout in terms of these performance issues.

# 7 Noise performance of preamplifier

The parrallel noise due to the parrallel resistance is much smaller than the other terms in equation 7 and so is frequently neglected. In this case if the diode at the input is replaced by a capacitor $C_{in}$, equation 7 becomes

$$ENC = a + b.C_{in} \tag{8}$$

The constant a depends on the intrinsic capacitance of the FET and b is inversely proportional to the root of the transconductance. It is customary to quote a and b to indicate the performance of the preamplifier. Figure 5 shows the ENC versus input capacitance for the preamplifier. A shaping time of 2 $\mu$s is used (the choice of shaping time is discussed later). We use a Canberra 2021 shaping amplifier for our tests. A custom shaper/postamplifier will be incorporated on the final preamplifier card but this will not alter the quoted noise performance. A constant of 256 $e^-$ and a gradient of 1.7 $e^-$ per pF is obtained. For completeness we note that the parrallel resistance is 70 M$\Omega$ which gives a noise of 130 $e^-$To be completely accurate this should be subracted in quadrature from each point in figure 5 before fitting. In this case a constant of 220 and a gradient of 1.8 $e^-$ per pF is obtained.

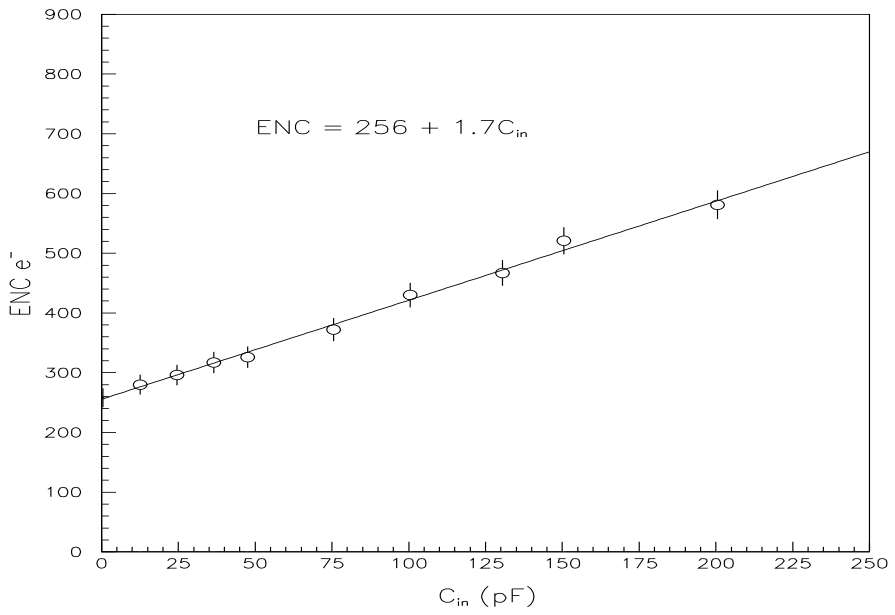


Figure 5: Noise performance of *BABAR* preamplifier.

This compares favorably with preamplifiers used for similar detectors [4], [3]. The FET used is a Hitachi 2SK190 which has $C_{gs} = 75$ pF, $g_m = 45$ mS. Note that the transconductance, $g_m$, is set by the choice of drain-source current in

the FET and so by increasing this current one can decrease the noise. However the increased current causes increased power dissipation which requires additional cooling in the detector. The drain-source operating current is 5 mA which results in a power dissipation of 30 mW per channel.

# 8 Options for Crystal- Photodiode coupling

There are two possibilities for coupling the crystal to the photodiode. They both use the same preamplifier. However the options use different diodes and so the light yield and noise performance are different.

## 8.1 Wavelength shifter Option

It is possible to couple the crystal to the photodetector by using a planar wavelength shifter (WLS) that covers the entire rear face of the crystal (figure 2). The thickness of the WLS is 3.4 mm which is determined by the active area of the two thin 3.4mm $\times$ 30 mm photodiodes epoxied to adjacent edges. The light entering the shifter is absorbed by the fluorescent dye molecules and then re-emitted isotropically and at a longer wavelength. The re-emitted light is internally reflected in the plane of the shifter and concentrated along the edges where the diodes are mounted. The wavelength shifting action enhances this transmission by preventing reabsorbtion and and also shifts the light to a region of higher diode quantum efficiency. The WLS is mounted on small standoffs in order to create an airgap which reduces the fraction of re-emitted light which returns to the crystal.

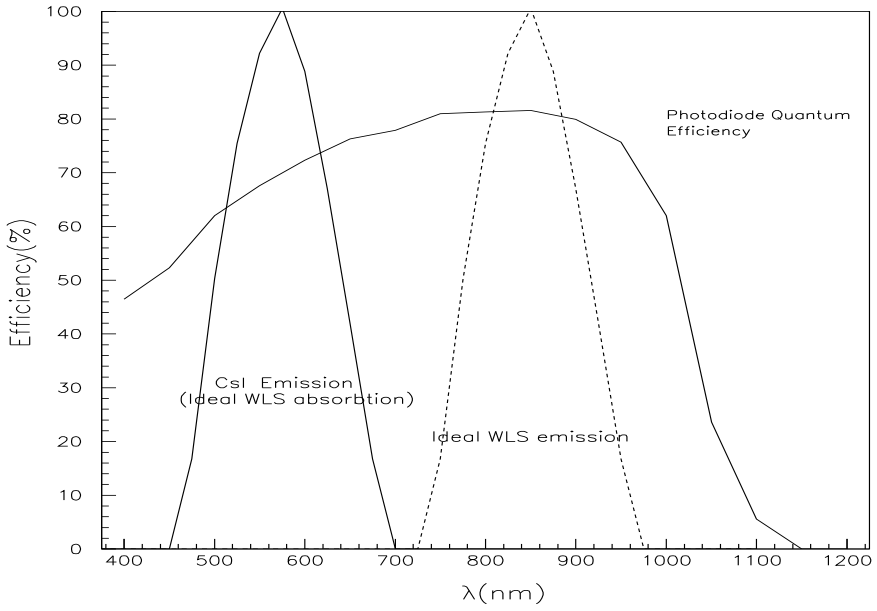


Figure 6: Photodiode sensitivity compared to CsI(Th) emission spectrum. Also shown is the ideal aborbtion and emission spectra of the wavelength shifter (WLS). The ideal absorption spectra is the same as the CsI(Th) emission spectra.

Figure 6 shows the spectral sensitivity of the photodiodes compared to the emission spectrum of CsI. Also shown is the shifted spectra from an ideal WLS. It is concentrated at the maxima of the diode quantum efficiency (approx 850 nm). The ideal absorption spectra of the WLS would encompass all of the CsI emission spectra yet have no overlap with the absorption spectra so that no re-absorption occurs. In addition the quantum efficiency of the WLS should be as high as possible. The WLS consists of a fluorescent dye captured in a plastic matrix. We have tested a variety of dyes and to date the best performance has been achieved with either a Crystal Barrel WLS which is BASF luminogen dye #339 in PMMA or with a dye manufactured by GlassFlex. Figure 7 shows the absorption and emission spectra for these dyes. We are currently evaluating different laser dyes which have close to

ideal wavelength shifting action. However the quantum efficiencies and ease of dissolving these dyes in a suitable plastic matrix present some problems.

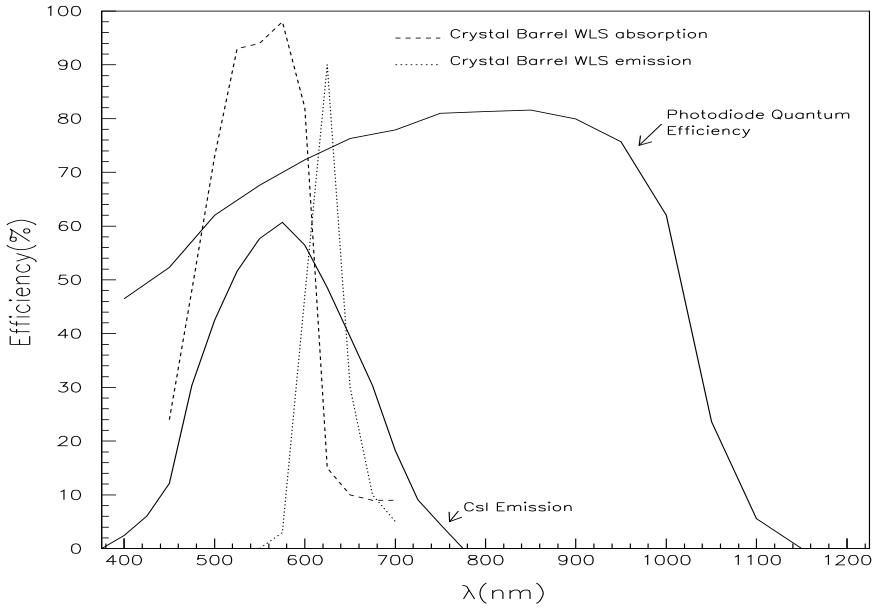


Figure 7: Emission and absorption spectra of WLS used for Crystal Barrel experiment. Also shown is the sensitivity of the photodiode and the CsI(Th) emission spectrum.

The WLS edges and faces not exposed to the crystal are covered in white diffuse reflector to minimize light loss. This improves the light yield by 5-10 %.

### 8.1.1 Electronic Noise Performance of WLS Option

The two photodiodes are readout with separate preamplifiers and Canberra 2021 shaping amplifiers as in figure 1. The digitization is done with a 12 bit 10 MHz waveform digitizer (FADC) manufactured by Joerger. The DAQ is a VME based system controlled by a Mac with VXI interface. The DAQ sofware is written using the Labview Graphic programming system. The two channels are summed in software after pedestal subtraction and gain

correction. The summation doubles the signal. The intrinsic electronic noise is summed incoherently and so increases by a factor $\sqrt{2}$. The resultant equivalent noise energy is then decreased by a factor $\sqrt{2}$. This setup closely mimics the actual detector configuration.

The 3.4mm $\times$ 30 mm diodes are commercially available in three different depletion layer depths of 200,300 and 500 $\mu$m. The diodes are covered with a protective layer of SiO and transparent epoxy resin and packaged in a white ceramic shell. The quantum efficiency at the peak of spectral response is 80 %. The differing depletion layer depths give diodes of different capacitance and dark current. In addition the diode must be biased correctly to achieve full depletion and thus minimal noise (equations 6, 7). Figure 8 shows the equivalent noise charge versus bias voltage for two Hamamatsu 3588-03 (3.4 mm $\times$ 30mm $\times$ 300 $\mu$m). We use an operating point of 50 V. Figure 8 also shows the dependence of the noise on the shaping time. From equation 7 it can be seen that for low shaping time the capacitive noise is dominant and for larger shaping times the dark current noise is more significant. The operating shaping time of 2 $\mu$s is set by consideration of beam backgrounds that the calorimeter is likely to encounter at PEP-II. However this value also lies close to a minima and so gives near optimal noise performance. The ENC per crystal is 620 $e^-$ . This is equivalent to 440 $e^-$ per channel ($620/\sqrt{2}$). The capacitance at full depletion is 55 pF. From figure 7 this gives a noise of 350 $e^-$ from the thermal noise of the FET. The dark current is 4 nA and from the first term of equation 7 this implies a contribution of 315 $e^-$The incoherent sum of the two contributions is 470 $e^-$ in good agreement with the measured value of 440 $e^-$

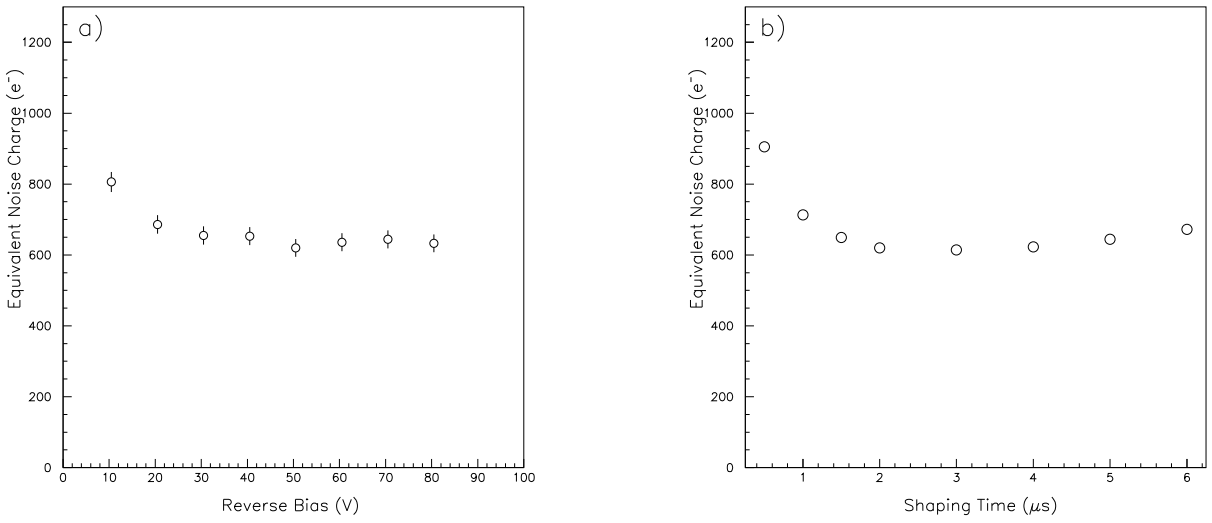


Figure 8: The dependence of equivalent noise charge per crystal on a) photodiode reverse bias voltage b) shaping time. The figures are for the sum of two 3588-03 (3.4 mm $\times$ 30mm $\times$ 300 $\mu$m ) appropriate for the WLS readout option.

We have in addition tested a thinner photodiode for this readout option (3.4 mm $\times$ 30mm $\times$ 200 $\mu$m). This has a lower dark current of 2 nA but this is offset by a higher capacitance of 80 pF. The dark current and thermal noise are 220 and 390 $e^-$ to give a total of 450 $e^-$ comparable to the 300 $\mu$m diode. Note that the dark current is very dependent on the temperature. Figure 9 shows the variation of noise with temperature for two 3588-03 (3.4 mm $\times$ 30mm $\times$ 300 $\mu$m) diodes. A reduction of 10 $^o$C reduces the noise to xxxx.

Figure 9: The noise versus temperature for the sum of two 3588-03 (3.4 mm $\times$ 30mm $\times$ 300 $\mu$ m ) photodiodes.

Further improvements in the electronic noise may come from different JFETs and the ongoing efforts of the diode manufactures to reduce dark current by increasing the purity of silicon. The replacement of the SiO protective layer with SiN may improve the quantum efficiency to the theoretical maximum of 90 %. The remaining 10 % is due to light being trapped by internal reflection in the epoxy resin layer. The removal of this layer would seriously compromise the reliability. The photodiodes are epoxied to the WLS using a standard epoxy such as Kodak HE-80. The structure of this bond must be optimized as burrs at the edges of the bond may cause refraction of light away from the diode. Simple modifications of the diode packaging, such as orienting the wire bonds at $90^o$ to the diode to facilitate connection to the preamplifier board which is mounted directly behind the WLS are possible without incurring substantial cost increases. The diodes are cut from circular silicon wafers 7cm in diameter and so it is possible to manufacture a diode to cover the entire edge of the WLS, although the cost increase and time required to develop to existing reliability standards may be prohibitive.

### 8.1.2 Light Yield of WLS option

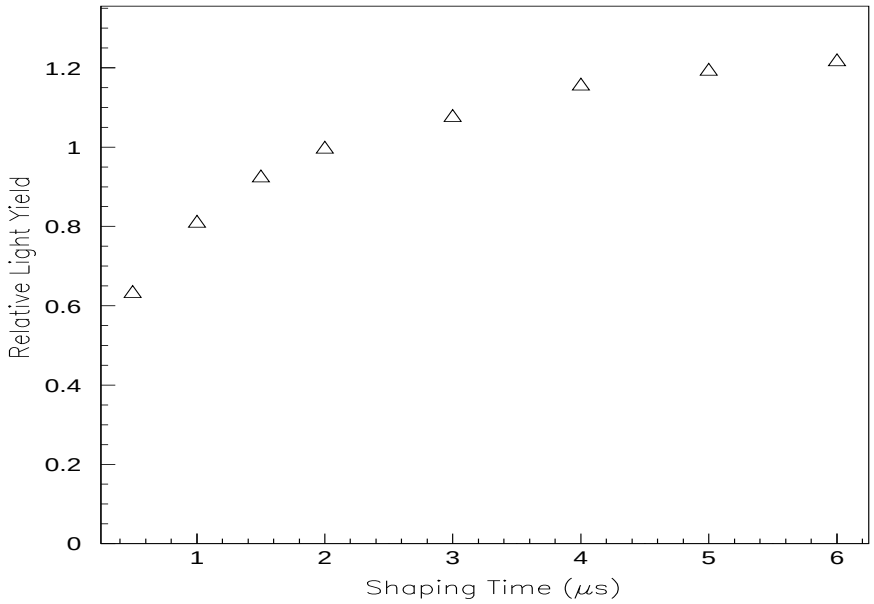


Figure 10: The relative light yield versus shaping time for either readout option.

The light yield is measured using a collimated $^{22}$Na source which has two lines at 512 and 1275 keV. The source is placed 15 cm directly in front of the crystal. The light yield of WLS readout is 4600 pe/ MeV for the full sized Kharkov crystal described previously. Both the crystal Barrel and the Glassflex WLS give the same result. The equivalent noise energy is then 135 keV with an ENC of 620 $e^-$ . This is well within our noise specification. Table 1 gives the light yield for a variety of crystals using the WLS readout scheme. The ENE for each case can be evaluated using equation 4. We have used a shaping time of 2 $\mu$S. Beam related backgrounds may require a slightly shorter time. Figure 10 shows how the relative light yield changes with shaping time. The ENE may then be estimated using figure 8 to scale the noise.

| Vendor | Front Dim. ($cm^2$) | Rear Dim. ($cm^2$) | Length (cm) | LY Rel. to Std (%) | LY Direct ($pe$/MeV) | LY WLS ($pe$/MeV) |
|---|---|---|---|---|---|---|
| Kharkov | 25 | 25 | 34 | 32 | 6340 | 4200 |
| Kharkov | 34 | 20 | 34 | 32 | 5960 | 4600 |
| Crismatec | 28 | 18 | 23 | 27 | 4820 | 3650 |
| Crismatec(hex) | 28 | 18 | 22 | 31 | 5300 | 4250 |
| Horiba | 28 | 18 | 23 | 40 | 8600 | 5560 |
| Horiba(hex) | 28 | 18 | 23 | 50 | 9800 | 6800 |
| Polsyscine | 34 | 20 | 34 | 35 | 6500 | 4550 |

Table 1: Light yield (LY) measurements (as described in the text) for full-sized crystals. All crystals have a square crossection except where indicated.

## 8.2 Direct readout Option

An alternative readout option, which has been successfully employed at CLEOII [3], is to mount the diodes on a lucite or silicon cookie sheet which is then directly epoxied to the crystal (figure 2). As there is no concentration of the light this requires a larger photodiode area to achieve the same light yield as the WLS option. In the following test we use Bicron optical grease as the optical coupling rather than a silicon cookie. The light transmission is identical.

### 8.2.1 Noise Performance of Direct Option

The larger area increases the dark current and capacitance of the photodiodes and so implies an increased noise. There are three possible configurations , four 10 mm $\times$ 10 mm photodiodes, two 20 mm $\times$ 10 mm, and two 18 mm $\times$ 18 mm. However, the prohibitive cost of these solutions limits the possible configuration to two 20 mm $\times$ 10 mm $\times$ 300 $\mu$m. Figure 11 shows the noise versus bias voltage and versus shaping time for this option using two Hamamatsu 2744-03 photodiodes. At 50V, 2$\mu$s the noise is 680 $e^-$The capacitance at this voltage is 100 pF and the dark current is 4 nA to give noise contributions of 420 $e^-$ and 315 $e^-$ respectively. Figure 9 shows the

noise versus temperature for this solution.

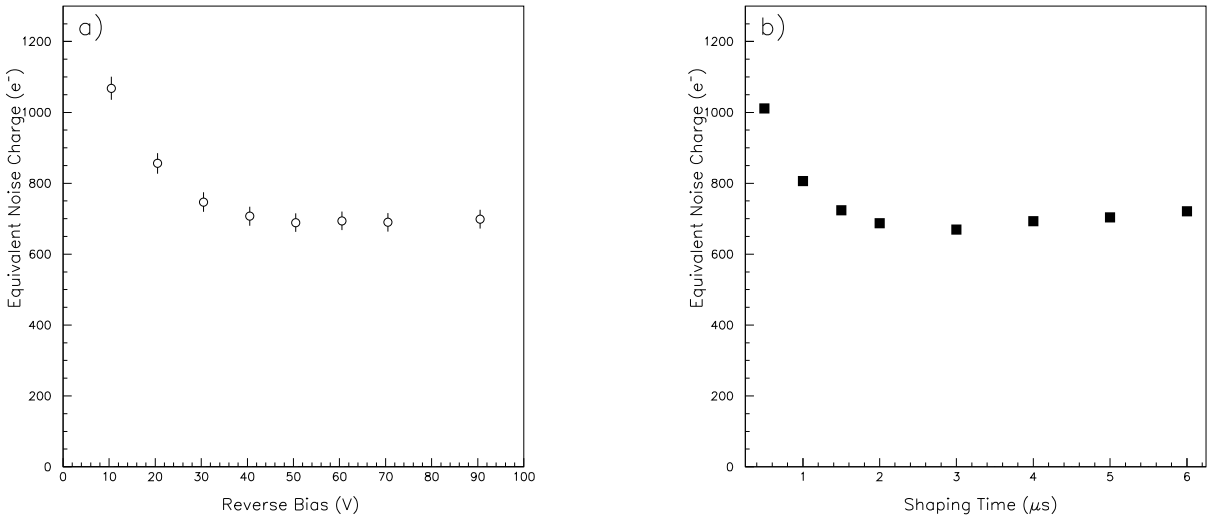


Figure 11: The dependence of equivalent noise charge per crystal on a) photodiode reverse bias voltage b) shaping time. The figures are for the sum of two Hamamatsu 2744-03 (20 mm $\times$ 10mm $\times$ 300 $\mu$m ).

### 8.2.2 Light Yield of Direct readout

For the full sized Kharkov crystal described previously we measure a light yield of 5960 pe/ MeVusing two Hamamatsu 2744-03 photodiodes (20 mm $\times$ 10 mm $\times$ 300 $\mu$m). The ENC is 680 $e^-$The ENE is then 114 keV. Table 1 gives the light yields for a variety of crystals using the direct readout solution. The light yield and noise may be scaled for different shaping times using figures 11, 10.

# 9 Conclusions

We have set a target of 150 keV incoherent noise with a dual redundancy front end readout system. We have developed a low noise preamplifier and

tested it with two possible readout schemes. The wavelength shifter solution has an electronic noise charge of 620 $e^-$ and gives a light yield of 4600 $e^-$ with a full size, good quality Kharkov crystal. This results in an equivalent noise energy of 135 keV . The direct solution gives an ENC of 680 $e^-$ and a light yield of 5960 pe/ MeVfor the same crystal. The ENE is 114 keVÀssuming that crystals of similar quality can be obtained in large quantities then either solution meets our requirement. The cost of the larger diodes used for the direct solution is twice that of the smaller diodes used for the WLS solution. In addition since the WLS covers the entire face of the crystal it is insensitive to any non-uniformities in light yield across this area. The WLS cost is small compared to the diodes. The WLS is photochemically stable and crystal barrel has seen no effects due to radiation damage.

# 10 Acknowledgement

R. Zhu, CALTECH has achieved similar results with the direct readout and provided valuable help and advice for this work.

# References

[1] C. Jessop *et al.* "Reliability Issues for CsI Calorimeter", *BABAR* Note #217, 1994.

[2] R. Wang *et al.* "Crystal Wrapping Studies", *BABAR* Note #212, 1994.

[3] C. Bebek CLEO collaboration Nucl. Instrum. Methods **265**, 258 (1988)

[4] E. Aker *et al.*Crystal Barrel Collaboration CERN-PPE/92-126

[5] R. Baggs *et al.* Tau/Charm Collaboration *Nucl. Instr. Meth.* **344**, 547 (1994).

[6] Dr. Yamamoto, Hamamatsu Corporation, Japan. Private communication